

# Micro- and Nanomorphologies of Isotactic Polystyrene Revealed by PLM, AFM, and TEM

Tianxi Liu,<sup>1</sup> Kuixiang Ma,<sup>1</sup> Zhehui Liu,<sup>1</sup> Chaobin He,<sup>1</sup> Tai-Shung Chung<sup>2</sup>

<sup>1</sup> Institute of Materials Research and Engineering, 3 Research Link, Singapore 117602

<sup>2</sup> Department of Chemical and Environmental Engineering, National University of Singapore, 10 Kent Ridge, Singapore 119260

Received 11 October 2001; accepted 14 December 2001

**ABSTRACT:** The spherulitic and lamellar morphologies of isotactic polystyrene (iPS) isothermally crystallized from the glassy state were investigated by polarized light microscopy (PLM), atomic force microscopy (AFM), and transmission electron microscopy (TEM). The AFM phase images and TEM bright-field electron micrographs revealed that the iPS spherulites consist of a number of dominant edge-on lamellae which continuously grow outward by splaying and branching. By partial melting, the less perfect subsidiary

lamellae, which are formed within the framework of the dominant ones due to the growth in restricted spaces and possess lower thermal stability than that of the dominant ones, were directly observed by TEM. © 2002 Wiley Periodicals, Inc. *J Appl Polym Sci* 86: 422–427, 2002

**Key words:** isotactic polystyrene; morphology; PLM; AFM; TEM

## INTRODUCTION

In 1945, spherulites were reported in polyethylene (PE) and have been recognized as being characteristic of quiescent crystallization of macromolecules from their melts.<sup>1</sup> They have been assumed to be of particular importance for crystalline polymers such as PE, polypropylene (PP), and isotactic polystyrene (iPS), in which they are the characteristic mode of growth from the melt and a principal determinant of properties for final products. However, the internal organization of spherulites and the processes which produce them have long been unsolved major problems of crystal growth.<sup>1</sup> What is unclear from models of polymer crystallization is how growth progresses and how lamellae interact when they come into contact with each other.<sup>2</sup> These initially puzzling issues can be ascertained with the advent of systemic studies at the lamellar level using electron microscopy for melt-crystallized polymers.<sup>3</sup>

Bassett et al. used transmission electron microscopy (TEM) following a permanganic etching and replication technique to investigate the crystalline morphologies of polymers, such as PE, iPS, and PP.<sup>4–6</sup> Their results showed that there are two dis-

tinct types of lamellar crystals present in the spherulites. Dominant, or leading, lamellae could be characterized by a thicker appearance and were identified as growing first to provide a skeleton for the spherulites. Secondary, or in-filling, lamellae were seen as being rather thinner and having an ill-defined orientation within the spherulites. These secondary lamellae were taken to have grown behind the main growth front, after the dominant lamellae, and served to fill in the spaces between the primary, leading lamellae. Most recently, using atomic force microscopy (AFM), Li et al. showed that secondary lamellae, which give rise to the curvature in a spherulite, form through branching caused by secondary nuclei that originate from leftover chain segments trapped in the parent lamellae (cilia).<sup>7,8</sup> Upon impingement of two growing lamellae, crystalline growth does not necessarily halt.

Specific to iPS, recently, there has been significant interest in understanding the mechanisms of crystallization because of its potential commercial applications.<sup>9–13</sup> Despite wide applications of AFM in various polymeric systems in recent years,<sup>14</sup> to our knowledge, few AFM studies have been reported on the spherulitic morphology of iPS. In addition, the sample preparation for surface replication for TEM observation is quite tedious and time-consuming. The main objective of this study was to investigate, comparatively, the spherulitic morphologies of cold-crystallized iPS on micro- and nanoscales using optical microscopy, AFM, and TEM. Most significantly, the ex-

Correspondence to: T. Liu (liu-tx@imre.org.sg).

Dedicated in memory to Prof. Dr. Juergen Petermann (University of Dortmund, Germany) who passed away on May 20, 2001.

istence and melting of subsidiary lamellae was visualized by direct TEM observations.

### EXPERIMENTAL

The powdery iPS sample ( $M_w = 752,000$ ; isotacticity: 97%) was purchased from Polymer Laboratories. The film used for optical microscopic observation was prepared by melting (at 250°C for 5 min) and pressing the sample (sandwiched between two microscope slides) and then quenching in ice water. The obtained amorphous film samples (with thickness about 40–50  $\mu\text{m}$ ) were transferred onto a hot stage for isothermal crystallization at 160°C for 6 h. A Leitz DMRB polarized light microscope (PLM) was used to investigate the crystalline morphology at the micron level.

The dilute polymer-xylene solution (with a concentration of 0.5% w/v) was cast onto freshly cleaved mica. After the evaporation of the solvent, the obtained film experienced the same thermal history as that used in the PLM experiment. The AFM observations of the surface morphology for the obtained crystalline film were carried out on an AutoProbe CP Research model, supplied by ThermoMicroscopes operating in ambient. Both height (topography) and phase images were obtained simultaneously under an intermittent contact mode using a 100- $\mu\text{m}$  scanner and an AutoProbe mounted Si tip with a force constant of 3.2 N/m and a frequency of 90 kHz, respectively. The images presented here were processed by flattening with IP 1.3 Imaging Processing software, provided by the manufacturer.

Thin films for direct TEM observations were obtained by the following procedure: First, the dilute polymer-xylene solution (with a concentration of 0.1% w/v) was dropped onto mica covered with a carbon film; then, after the evaporation of the solvent, the polymer films on the carbon-support film were floated onto the water surface and then transferred onto electron microscope copper grids. Subsequently, the obtained thin films on the grids underwent the same thermal treatment as described above. Morphological observations were carried out using a Philips CM200 TEM operated at 200 kV, and the contrast in the bright-field (BF) electron micrographs of the thin films was obtained by the objective-lens defocus contrast method of about 40  $\mu\text{m}$ . This technique was first introduced by Petermann and Gleiter.<sup>15</sup>

## RESULTS AND DISCUSSION

### Spherulitic and lamellar morphologies by PLM and AFM

It has been well known that the crystallization of polymers from the melt can yield a wealth of morpho-

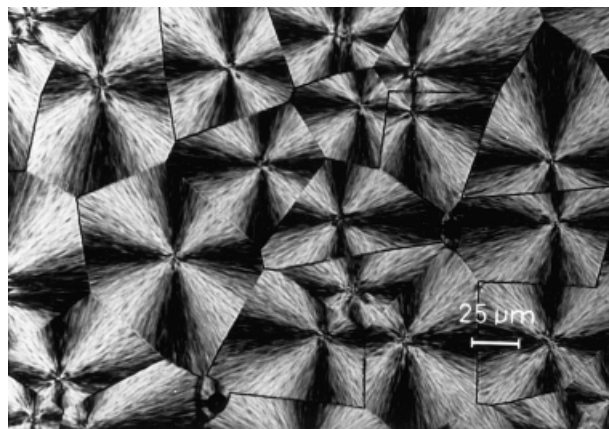


**Figure 1** PLM micrograph of an iPS sample isothermally crystallized at 160°C for 6 h from the glassy state.

logical forms. The most common one would be a spherulite, a spherically symmetric array of lamellar crystals. In the case of the iPS system, such a typical spherulitic morphology can also be observed upon crystallization from the glassy state, due to its slow crystallization rate. But for most crystalline polymers, while crystallizing from the amorphous state, usually numerous small crystals will be randomly formed due to high nucleation density. It is therefore difficult to form perfect crystals with large sizes for the cold crystallization. However, for iPS, the case is very different. A typical PLM micrograph of iPS isothermally crystallized at 160°C for 6 h from the glassy state is presented in Figure 1. The well-developed spherulites were clearly observed owing to the difficulty of nucleation and the characteristic slow growth rate of iPS.<sup>16</sup> The spherulites have the characteristic of a continuous sheaflike texture aligning radially outward. Both the typical and pronounced Maltese cross extinction pattern and the sharp boundaries of spherulites were observed. This spherulitic morphology observed in cold-crystallized iPS is in contrast to the crystalline morphology in syndiotactic polystyrene (sPS) crystallized from the amorphous glassy state visualized by PLM and TEM. The latter usually exhibits irregular micellar-type lamellae (not spherulite) with a random lamellar orientation, probably owing to its fast crystallization rate compared with iPS.<sup>16</sup> In addition, the spherulitic morphologies of iPS vary considerably in appearance depending on the crystallization temperature or undercooling. For instance, the spherulites become coarser in texture and the Maltese cross extinction patterns are obviously blurred at lower undercooling.<sup>17</sup>

The resolution of light microscopy (which is used to access the macroscopic crystalline texture of polymers) is not sufficient for the observations of the internal organization in polymer spherulites. In this re-

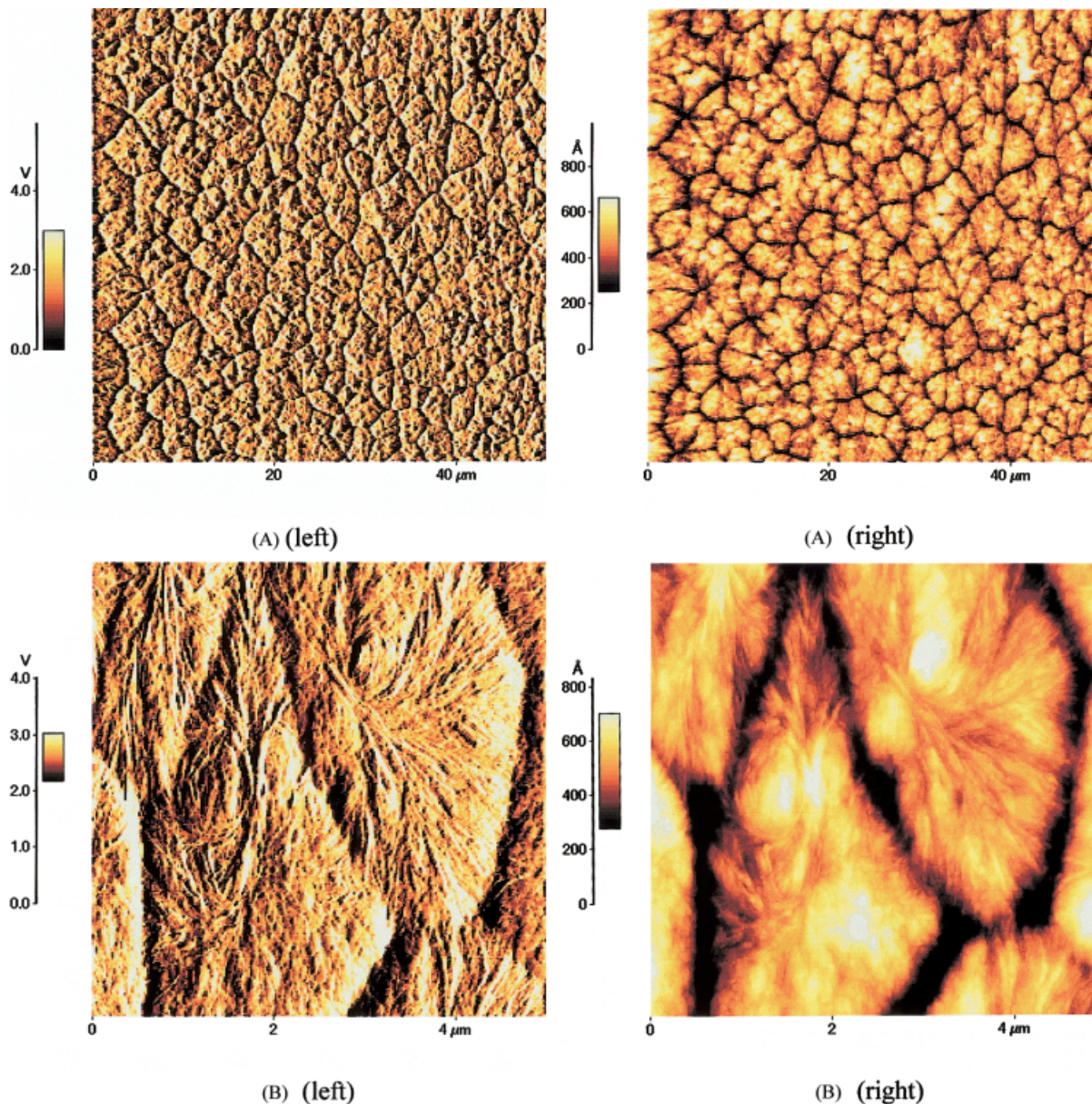


**Figure 2** Noncontact AFM (right) height and (left) phase images of an iPS solution-casting film having the same thermal history as in Figure 1. The fields of view are (A)  $50 \times 50 \mu\text{m}$  and (B)  $5 \times 5 \mu\text{m}$ .

gard, AFM has the resolution required to elucidate polymer microstructural features on the nanoscale. Simultaneously obtained AFM height and phase images for cold-crystallized iPS are presented in Figure 2. From the lower magnification photographs [Fig. 2(A)], it can be seen that numerous spherulites were observed with distinct impinged boundaries. In contrast to the sharp boundaries between the spherulites observed by PLM, the interspherulitic regions become more pronounced under AFM observation. It is known that the basis for the phenomenon of spherulitic crystallization is the tendency for the polymer to reject noncrystallizable material from the crystallization front during their formation.<sup>18</sup> As a result, the

boundaries between adjacent spherulites contain a high concentration of noncrystallizable material composed of low molecular weight chains, atactic polymer, and various impurities. In principle, the molecules in the used iPS samples with low molecular weight and stereoregularity (containing 3% chain structural irregularities in the used iPS) are rejected preferentially by growing crystals due to the fractionation or segregation effects during crystallization.

Under large magnification [Fig. 2(B)], it is clearly observed that the hard crystalline lamellae are surrounded by certain softer (darker) amorphous phase regions due to the contrast between crystal and interlamellar noncrystalline layer spacings. The spherulitic

structures (with a central “binocularlike” open space) consisting of closely packed edge-on lamellae especially for the outer regions are well recognized. Additionally, a number of single-crystal-like platelets (flat-on lamellae) can also be clearly seen in the open regions, particularly within the spherulitic “eyes” on either side of the nuclei. In general, phase data are more precise for resolving lamellar dimensions and boundaries, even though the qualitative information is similar.

### Morphological observations and lamellar melting by TEM

For semicrystalline iPS which consists of crystalline entities and their amorphous surroundings, a proper amount of objective-lens defocus in the BF imaging mode in TEM observation gives sufficient “phase contrast” to the image, owing to the difference in the electrostatic inner potential.<sup>15</sup> Figure 3 shows the TEM BF micrograph of an iPS thin-film sample cold-crystallized at 160°C for 6 h. It can be clearly seen that, using phase contrast in undefocus conditions, the darker contrast correlates to the higher-density or crystalline areas, and the brighter contrast, to the lower-density or amorphous areas. The well-developed spherulitic structures consisting of closely packed edge-on lamellae are the main characteristic morphology. A number of lamellar stacks radically grow outward from the central regions, a structure roughly parallel and centrally connected, by splaying, branching, and bending that leads to a spherical envelope. The spherulites develop in the classical way from individual units via lamellar branching to quasi-spherical symmetry. The primary cause of splaying between adjacent lamellae is the pressure of uncrystallized (compressed) molecular cilia.<sup>19,20</sup> Close inspection of the micrograph indicates that both curved lamellae and

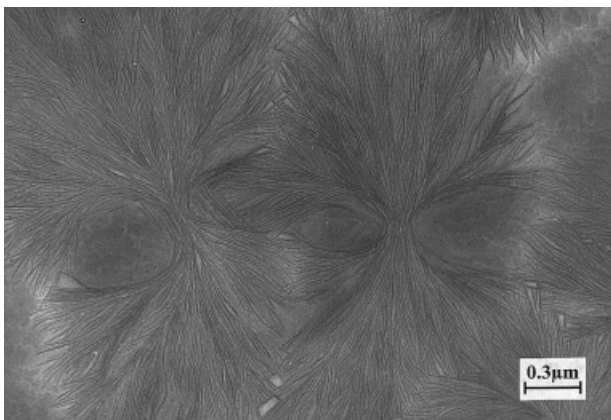


**Figure 3** TEM BF electron micrograph of an iPS film having the same thermal history as that in Figure 1.

some near square “holes” are formed due to splaying, branching, and the impingement of the growing lamellae, especially in the outer regions of the spherulites. In some areas, however, the growing lamellae do not stop after impingement but further grow to form the “crossed” lamellar structures. Our TEM observations evidently support the arguments based on recent AFM observations by Li et al. that crystal growth does not necessarily halt upon impingement of two lamellae.<sup>7,8</sup>

Furthermore, close inspection of the micrograph also indicates that the shape, size, and contrast along the individual lamella (the so-called dominant lamellae) vary over the whole spherulite. There exist some less perfect and/or thinner subsidiary lamellae observed by a somewhat weaker phase (defocus) image contrast in the TEM. These subsidiary lamellae (i.e., the later-crystallizing lamellae) probably consist of some defective crystals containing lattice defects, surface constraints, and other irregularities, which may not have enough space to grow and may be restricted within the framework of the dominant lamellae. This morphology may be formed by the gradual branching and splaying growth of individual dominant lamellae followed by in-filling subsidiary growth. Given repetitive branching, generally at giant screw dislocations and sufficient space, eventually the structure closes, yielding central “eyelets” around the splaying axis. The exact mechanism by which this splaying manifests itself is still not certain. Two possible explanations are the compression resulting from the uncrystallized molecular portions of cilia confined between lamellae, that is, molecules protruding on the faces of adjacent lamellae, and reptation forces.<sup>19–23</sup>

In our previous reports,<sup>24–26</sup> it was shown that the thermal stability within an individual lamella is not uniform due to structural fluctuation as reflected by the fragmentation of lamellae upon thermally treating at different temperatures. The less perfect domains along single lamella serve as melting nuclei. To confirm the presence of the subsidiary lamellae from the morphological point of view and to further reveal the internal architecture of the spherulites, partial melting experiments are performed. Typically, the initially crystalline samples are further treated at a temperature approaching the melting point ( $T_m = 220^\circ\text{C}$ ) for a short time (e.g., 1 min) and then rapidly quenched to room temperature for the subsequent TEM observation. Figure 4(A,B) illustrates the morphological changes observed by TEM after the crystalline iPS thin films experienced partial melting at 210°C for 1 and 10 min, respectively. From Figure 4(A), it can be clearly observed that some lamellae with less thermal stability are melted, and only a few fractions (dominant lamellae) are

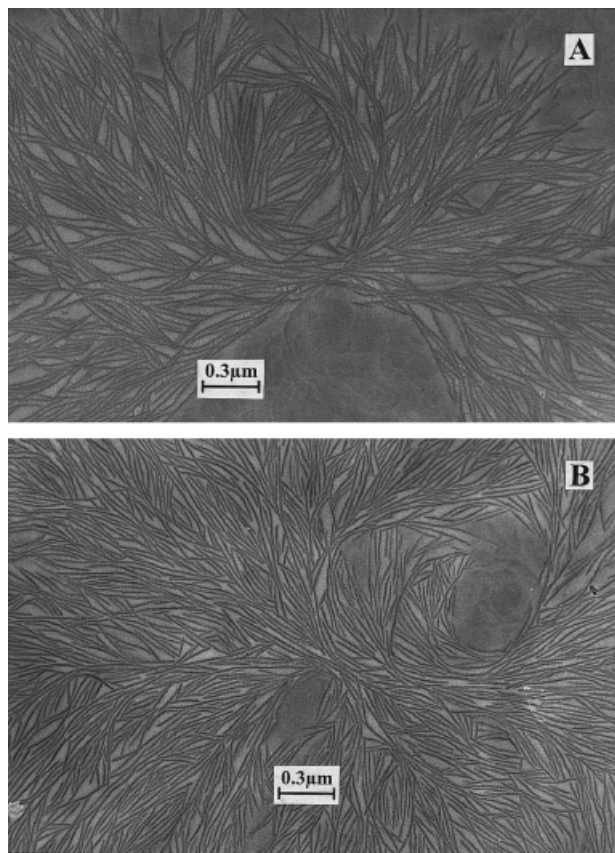


**Figure 4** TEM BF electron micrographs of the iPS thin films having the same thermal history as that in Figure 1, but further treated at 210°C for (A) 1 min and (B) 10 min, followed by rapidly quenching to room temperature.

left. Thus, the framework of dominant lamellae is especially clear in Figure 4(A). Moreover, close inspection shows that some small residual spots or granules still remain between the stable lamellae, indicating the last traces of the melting of the subsidiary lamellae with less thermal stability.

To study the possibility of reorganization (i.e., melting and recrystallization) after partial melting, the originally crystalline sample is kept at 210°C for a long period of time, for instance, 10 min. As illustrated in Figure 4(B), three main features can be observed: (1) The residual granular lamellae between the dominant ones completely disappear, indicating the complete melting of subsidiary lamellae; (2) the lengths of the remaining lamellae, to some extent, decrease compared with those in Figure 4(A) (1 min), illustrating the occurrence of lamellar fragmentation<sup>26,27</sup>; and (3) under the used conditions (210°C for 10 min), recrystallization (not melting) dominates the whole reorganization process, being reflected by the formation of many recrystallized lamellae [Fig. 4(B)]. The rate of such a recrystallization is much faster than that of the initial crystallization process. Some other hot but open

issues in this respect remain, such as: How much faster is the recrystallization rate than the crystallization one? Do the recrystallized lamellae grow along the paths of the original ones? What happens when two *recrystallized* lamellae approach or impinge on each other? The fundamental research on these important and interesting topics is still in progress in our laboratory.

## CONCLUSIONS

The micro- and nanomorphologies of iPS were studied by optical microscopy, AFM, and TEM. Using partial melting experiments, the internal architecture of iPS spherulites were directly visualized by TEM (using the objective-lens defocus contrast method). The iPS spherulites consist of two lamellar populations with different thermal stability: perfect or stable dominant lamellae and less perfect or less stable subsidiary lamellae. In addition, the lamellar melting and recrystallization behavior was observed on a nanoscale using TEM.

The TEM experiments were carried out in Prof. J. Petermann's group (University of Dortmund). One of the authors (T. L.) is grateful to the Alexander von Humboldt Foundation for granting him a research stipend during his stay in Germany and the initiation of the subject by Prof. Petermann.

## References

- Keller, A. *Growth and Perfection of Crystals*; Wiley-Interscience: New York, 1958; p 499.
- Lavine, M. *S. Science* 2001, 291, 949.
- Abo el Maaty, M. I.; Hosier, I. L.; Bassett, D. C. *Macromolecules* 1998, 31, 153.
- Bassett, D. C.; Vaughan, A. S. *Polymer* 1995, 26, 717.
- Vaughan, A. S.; Bassett, D. C. *Polymer* 1988, 29, 1397.
- Vaughan, A. S.; Bassett, D. C. *Comprehensive Polymer Science*; Pergamon: New York, 1989; Vol. 2, Chapter 12, pp 415–457.
- Li, L.; Chan, C. M.; Li, J. X.; Ng, K. M.; Yeung, K. L.; Weng, L. T. *Macromolecules* 1999, 32, 8240.
- Li, L.; Chan, C. M.; Yeung, K. L.; Li, J. X.; Ng, K. M.; Lei, Y. *Macromolecules* 2001, 34, 316.
- Vittoria, V.; Petrillo, E.; Russo, R. *J Macromol Sci Phys B* 1996, 35, 147.
- Petrillo, E.; Russo, R.; D'Aniello, C.; Vittoria, V. *J Macromol Sci Phys B* 1998, 37, 15.
- Kimura, T.; Ezure, H.; Tanaka, S.; Ito, E. *J Polym Sci Polym Phys* 1998, 36, 1227.
- Matsuba, G.; Kaji, K.; Nishida, K.; Kanaya, T.; Imai, M. *Polym J* 1999, 31, 722.
- Ezura, H.; Kimura, T.; Ogawa, S.; Ito, E. *Macromolecules* 1997, 30, 3600.
- Magonov, S. N.; Reneker, R. H. *Annu Rev Mater Sci* 1997, 27, 175.
- Petermann, J.; Gleiter, H. *Philos Mag* 1975, 31, 929.
- Liu, T. X., manuscript in preparation.
- Liu, T. X.; Xiao, Q., manuscript in preparation.
- Keith, H. D.; Padden, F. J. *J Appl Phys* 1964, 35, 1270.

19. Bassett, D. C.; Mitsuhashi, S.; Keller, A. *J Polym Sci A* 1963, 1, 73.
20. Patel, D.; Bassett, D. C. *Proc R Soc Lond A* 1994, 445, 577.
21. Bassett, D. C. *Principles of Polymer Morphology*; Cambridge University: London, 1981.
22. Geil, P. H. *Growth and Perfection of Crystals*; Wiley: New York, 1958.
23. Wunderlich, B. *Macromolecular Physics*; Academic: New York, 1973; Vol. 1.
24. Liu, T. X.; Yan, S. K.; Bonnet, M.; Lieberwirth, I.; Rogausch, K. D.; Petermann, J. *J Mater Sci* 2000, 35, 5047.
25. Liu, T. X.; Petermann, J. *Polymer* 2001, 42, 6453.
26. Liu, T. X.; Petermann, J.; He, C. B.; Liu, Z. H.; Chung, T. S. *Macromolecules* 2001, 34, 4305.
27. Zhou, W.; Cheng, S. Z. D.; Putthanarat, S.; Eby, R. K.; Reneker, D. H.; Lotz, B.; Magonov, S.; Hsieh, E. T.; Geerts, R. G.; Palackal, S. J.; Hawley, G. R.; Welch, M. B. *Macromolecules* 2000, 33, 6861.